Elsevier Editorial System(tm) for Journal of Crystal Growth
Manuscript Draft

Manuscript Number:

Title: Three-dimensional simulation and analysis for heat transfer and flow field on micro-floating zone of LHPG with asymmetrical perturbation

Article Type: Special issue: 5th IWCGT

Section/Category: General subjects

Keywords: A1. Heat transfer, A1. Fluid flows, A2, Laser heated pedestal growth,, A2, Single crystal growth, B1. Yttrium compounds

Corresponding Author: Dr. Chia-Yao Lo, Ph.D.

Corresponding Author's Institution: National Taiwan Ocean University

First Author: Peng-Yi Chen, Ph.D.

Order of Authors: Peng-Yi Chen, Ph.D.; En-Ping Huang, Ph.D.; Chia-Yao Lo, Ph.D.

Abstract: In symmetrical conditions, micro-floating zone showed symmetrical double eddy flow field distribution. However when perturbation increases, the double eddy flow field will be symmetrical to the tilt, and finally presents an unstable flow field vibration. Our purpose is to study the influence of molten zone on shape (vapor-liquid and solid-liquid interfaces) and internal heat flow field caused by the tilts of CO2 laser heating ring and gravity field with space asymmetrical to the molten zone when the source rod and seed had slight deviation to the growth axis of LHPG system. The asymmetrical system frame of three-dimensional simulation is to add the conditions of diameter reduction ratio and laser heating, and modify Lan's thermocapillary floating numerical mode. In order to enhance the degree of simulation and presentation of a more realistic physical meaning we have completed the comparison of molten zone shape between the simulation and the experiment. The simulation result showed that the double eddy flow field present tilt in x-y plane at z=0. In addition, the flow field vector and equipotential lines of the vertical and horizontal flow field velocities are no longer symmetry at the central axial of the molten zone. The flow field mainly affected by the laser heating ring deviation and the influence decrease with the source rod scale and diameter reduction ratio reducing under setting the deviation parameters of laser heating and gravity field. The influence of gravity to the flow field is extremely not obvious. We also simulate the growth axis and the gravity field perpendicular to each other under 1000-□m-diameter source rod. When the surface tension is lowered (~ 500 dyn cm-1) vapor-liquid interface drooped in the direction of gravity field, leading to tilt in the solid-liquid interface. At this point the appropriate heating ring with reverse angle compensation will enable the solid-liquid interface to maintain symmetry, and help us to develop LHPG crystal fiber growth with good crystal quality along horizontal direction.

Dear Editors,

We are pleased to submit our manuscript entitled “Three-dimensional simulation and analysis for heat transfer and flow field on micro-floating zone of LHPG with asymmetrical perturbation” by P. Y. Chen, E. P. Huang, and C. Y. Lo, for possible publication in Journal of Crystal Growth.

In this work, we study the influence of molten zone on shape (vapor-liquid and solid-liquid interfaces) and internal heat flow field caused by the tilts of CO_2 laser heating ring and gravity field with space asymmetrical to the molten zone when the source rod and seed had slight deviation to the growth axis of LHPG system. The asymmetrical system frame of three-dimensional simulation is to add the conditions of diameter reduction ratio and laser heating, and modify Lan’s thermocapillary floating numerical mode. In order to enhance the degree of simulation and presentation of a more realistic physical meaning we have completed the comparison of molten zone shape between the simulation and the experiment. Therefore, the conditions of mass and energy conservation are satisfied preliminary. This section was published in 2011 ICMAT conference. The simulation result showed that the double eddy flow field present tilt in x-y plane at z=0. In addition, the flow field vector and equipotential lines of the vertical and horizontal flow field velocities are no longer symmetry at the central axial of the molten zone. The flow field mainly affected by the laser heating ring deviation and the influence decrease with the source rod scale and diameter reduction ratio reducing under setting the deviation parameters of laser heating and gravity field. The influence of gravity to the flow field is extremely not obvious. We also simulate the growth axis and the gravity field perpendicular to each other under 1000-μm-diameter source rod. When the surface tension is lowered (~ 500 dyn cm^{-1}) vapor-liquid interface drooped in the direction of gravity field, leading to tilt in the solid-liquid interface. At this point the appropriate heating ring with reverse angle compensation will enable the solid-liquid interface to maintain symmetry, and help us to develop LHPG crystal fiber growth with good crystal quality along horizontal direction. This manuscript is the authors' original work and has not been published nor has it been submitted simultaneously elsewhere. That all authors have checked the manuscript and have agreed to the submission.

We would be happy to provide additional information if needed.

Sincerely yours

Dr. Chia-Yao Lo

Corresponding Author:

Chia-Yao Lo

Email: cylo@mail.ntou.edu.tw

Address:

Institute of Optoelectronic Sciences, National Taiwan Ocean University, Keelung 20224, Taiwan

Tel: +886-2-24622192 ext. 6717; fax: +886 2 24634360.

Coauthor:

Peng-Yi Chen, email: x00008415@meiho.edu.tw

Tel.: +886-8-7799821 ext 6506; mobile: +886 -937-388-198

En-Ping Huang, email: x00010092@meiho.edu.tw

Tel.: +886-8-7799821 ext 6502

***Highlights**

1. The shape of molten zone can be affected by laser heating and gravity field with space asymmetrical perturbation according to the size of source rod, followed by the laser power level, and then followed by the reduction ratio.
2. We simulate the growth axis and the gravity field perpendicular to each other under 1000-μm-diameter source rod. When the surface tension is lowered (~ 500 dyn cm^{-1}) vapor-liquid interface drooped in the direction of gravity field, leading to tilt in the solid-liquid interface.
3. The simulation results will help us to develop the technology of LHPG with horizontal growth.

*Abstract

Three-dimensional simulation and analysis for heat transfer and flow field on micro-floating zone of LHPG with asymmetrical perturbation

Peng-Yi Chen[a], En-Ping Huang[a] and Chia-Yao Lo[b,*]

[a]*Department of Gemology, Meiho University, Pingtung 91202, Taiwan*

[b]*Institute of Optoelectronic Sciences, National Taiwan Ocean University, Keelung 20224, Taiwan*

Abstract

In symmetrical conditions, micro-floating zone showed symmetrical double eddy flow field distribution. However when perturbation increases, the double eddy flow field will be symmetrical to the tilt, and finally presents an unstable flow field vibration. Our purpose is to study the influence of molten zone on shape (vapor-liquid and solid-liquid interfaces) and internal heat flow field caused by the tilts of CO_2 laser heating ring and gravity field with space asymmetrical to the molten zone when the source rod and seed had slight deviation to the growth axis of LHPG system. The asymmetrical system frame of three-dimensional simulation is to add the conditions of diameter reduction ratio and laser heating, and modify Lan's thermocapillary floating numerical mode. In order to enhance the degree of simulation and presentation of a more realistic physical meaning we have completed the comparison of molten zone shape between the simulation and the experiment. The simulation result showed that the double eddy flow field present tilt in x-y plane at z=0. In addition, the flow field vector and equipotential lines of the vertical and horizontal flow field velocities are no longer symmetry at the central axial of the molten zone. The flow field mainly affected by the laser heating ring deviation and the influence decrease with the source rod scale and diameter reduction ratio reducing under setting the deviation parameters of laser heating and gravity field. The influence of gravity to the flow field is extremely not obvious. We also simulate the growth axis and the gravity field perpendicular to each other under 1000-μm-diameter source rod. When the surface tension is lowered (~ 500 dyn cm^{-1}) vapor-liquid interface drooped in the direction of gravity field, leading to tilt in the solid-liquid interface. At this point the appropriate heating ring with reverse angle compensation will enable the solid-liquid interface to maintain symmetry, and help us to develop LHPG crystal fiber growth with good crystal quality along horizontal direction.

Keywords: A1. Heat transfer, A1. Fluid flows, A2, Laser heated pedestal growth,, A2, Single crystal growth, B1. Yttrium compounds

---

Three-dimensional simulation and analysis for heat transfer and flow field on micro-floating zone of LHPG with asymmetrical perturbation

Peng-Yi Chen[a], En-Ping Huang[a] and Chia-Yao Lo[b,*]

[a]*Department of Gemology, Meiho University, Pingtung 91202, Taiwan*

[b]*Institute of Optoelectronic Sciences, National Taiwan Ocean University, Keelung 20224, Taiwan*

Abstract

In symmetrical conditions, micro-floating zone showed symmetrical double eddy flow field distribution. However when perturbation increases, the double eddy flow field will be symmetrical to the tilt, and finally presents an unstable flow field vibration. Our purpose is to study the influence of molten zone on shape (vapor-liquid and solid-liquid interfaces) and internal heat flow field caused by the tilts of CO_2 laser heating ring and gravity field with space asymmetrical to the molten zone when the source rod and seed had slight deviation to the growth axis of LHPG system. The asymmetrical system frame of three-dimensional simulation is to add the conditions of diameter reduction ratio and laser heating, and modify Lan's thermocapillary floating numerical mode. In order to enhance the degree of simulation and presentation of a more realistic physical meaning we have completed the comparison of molten zone shape between the simulation and the experiment. The simulation result showed that the double eddy flow field present tilt in x-y plane at z=0. In addition, the flow field vector and equipotential lines of the vertical and horizontal flow field velocities are no longer symmetry at the central axial of the molten zone. The flow field mainly affected by the laser heating ring deviation and the influence decrease with the source rod scale and diameter reduction ratio reducing under setting the deviation parameters of laser heating and gravity field. The influence of gravity to the flow field is extremely not obvious. We also simulate the growth axis and the gravity field perpendicular to each other under 1000-μm-diameter source rod. When the surface tension is lowered (~ 500 dyn cm^{-1}) vapor-liquid interface drooped in the direction of gravity field, leading to tilt in the solid-liquid interface. At this point the appropriate heating ring with reverse angle compensation will enable the solid-liquid interface to maintain symmetry, and help us to develop LHPG crystal fiber growth with good crystal quality along horizontal direction.

Keywords: A1. Heat transfer, A1. Fluid flows, A2, Laser heated pedestal growth,, A2, Single crystal growth, B1. Yttrium compounds

1. Introduction

Crystal fiber growth using LHPG method has many advantages, such as crucible free and rapid crystal growth [1]. Therefore it widely used in crystal fiber manufacturing process. However, in the preparation process, the relative position of source rod and seed easily lead to slight offset or tilt caused by the two rods were manually fixed in the clamps. This situation will lead to the CO_2 laser heating ring and gravity field deviation. Thus it will affect the shape of the molten zone interface and the flow field distribution in the molten zone, further result in the instability of crystal fiber quality. There will be help to develop a horizontal manufacturing process of LHPG with proper or symmetrical solid-liquid interface shape through laser heating ring deviation to compensate gravity field with larger deviation (close to horizontal direction) or some material with higher surface tension during the control of solid-liquid interface. Our simulation analysis is first experimental verification of the molten zone shape close agreement to enhance the degree of simulation. Therefore, the conditions of mass and energy conservation are satisfied preliminary. This section was published in 2011 ICMAT conference [2]. LHPG symmetrical type on the micro-floating zone is discussed in our previous study [3-5].

In this paper, we add the conditions of diameter reduction ratio and laser heating, and modify Lan's thermocapillary floating numerical mode [6-8]. The modified model is a calculating system of physical grid through a non-orthogonal body-fitting grid transforming and uses the control-volume finite-difference method. The simulation results of the program would be effective in the analysis of the shape of the molten zone after changing. In addition, the internal flow field distribution and heat transfer properties.

*Corresponding author. Tel.: +886 2 24622192 6717; fax: +886 2 24634360.

E-mail address: cylo@mail.ntou.edu.tw (C.-Y. Lo).

2. Experimental Approach and Mathematical Formulation

The source rods were 0.5 mol.% doped Cr:YAG that were <111> in crystal orientation and 500×500 μm^2 in cross section. A 10.6-μm laser system (Synrad Firest V40, 40 W full power) with an attenuator to adjust the laser power was the heat source to enter the growth chamber. Inside the chamber, the incident Gaussian laser beam was transformed into a ring-shaped semi-Gaussian beam by a reflaxicon. After the 45 degree planar mirror, the parabolidal mirror focuses the beam on the top end of the source rod as shown in Fig. 1. After diameter-reduction steps on the LHPG system, the crystal fibers with diameters of less than 500 μm were obtained. Then, the as-grown fiber was used as the source rod to draw the fiber again through the same LHPG system.

Owing to the heating method of LHPG is based on the CO_2 laser beam through a series of optical system frame, and the beam final projection to 39 degrees to focus on the center of growth chamber. Therefore, we modified Lan's three-dimensional thermocapillary floating numerical mode in laser heating and diameter reduction type. In the x-y plane, the angle of inclination to provide gravity field α = 0 ~ 3 degrees and the heating ring plane tilting angle θ = 0 ~ 3 degrees range as asymmetrical perturbation of space for study.The laser intensity profile on the miniature MZ is approximated as an asymmetrical Gaussian distribution,

$$I_a = A_q \exp\left[-\alpha \left(r/\gamma \right)_a^2 \right] \tag{1}$$

where A_q and γ_a are the amplitude and width $\left(1/e^2\right)$ of the Gaussian distribution at z = 0, respectively, and α_a is the beam-shape factor [3,4].The physical properties of YAG material and other related input parameters are shown in Table 1 [9]. The dimensionless variables are defined by scaling length with the feed rod diameter D_f, velocity with α_m/D_f ; pressure with $\rho_m\alpha_m^2$ m=D_f^2, and temperature with the melting point T_m, where α_m is the thermal diffusivity and ρ_m the melt density. The steady-state governing equations describing the convection and heat transport in the melt are required as follows:

$$\begin{aligned} &\nabla \cdot \vec{v} = 0 \\ &\vec{v} \cdot \nabla \vec{v} = -\nabla P + \Pr \nabla^2 \vec{v} - \Pr Ra_T \left(T - 1\right) \vec{e}_g \\ &\vec{v} \cdot \nabla T = \nabla^2 T \end{aligned} \tag{2}$$

where $\vec{v}$, P and T are the dimensionless velocity, pressure, and temperature, respectively. Also, $\mathrm{pr} = \nu_m/\alpha_m$ is the Prandtl number, where ν_m is the kinematic viscosity. The gravity direction $\vec{e}_g$ is the unit vector of gravity, which can be aligned $\left(\alpha=0^0\right)$ with or tilted $\left(\alpha=3^0\right)$ and the angle θ between heating ring plane and the horizontal plane can be adjusted from $\left(\theta=0^0\right)$ to $\left(\theta=3^0\right)$ (from the growth axis on the x-y plane, as shown in Fig. 1. Furthermore, Tm also serves as a reference temperature. The associated dimensionless number in the source term of Eq. (2) is the thermal Rayleigh number, defined as follows:

$$Ra_T = \beta_T g T_m D_f^3 / \nu_m \alpha_m , \tag{3}$$

where β_T is the thermal expansion coefficients and g the gravitational acceleration. In the crystal (c) and the feed rod (f) only heat transfer needs to be considered:

$$v_i \vec{e}_x \nabla T = \nabla \cdot k_i \nabla T, \; i = (c, f) \tag{4}$$

where *r* is $k_i = \alpha_i(T)/\alpha_m$ the dimensionless thermal diffusivity of feed and crystal; α_i is the thermal diffusivity of the feed rod $(i = f)$ or the crystal $(i = c)$. Also, $\vec{e}_x$ is the unit vectors in the axial direction. In addition, most of the oxide crystals are often quite transparent to infrared. Therefore, internal radiation cannot be ignored. We have chosen the simplest model, i.e., the no-slip Rosseland diffusion model used by Vizman et al., for the crystal. Because the feed rod is usually prepared by sintering, the optical distance is small so that opacity is assumed; the melt is assumed to be opaque as well. One may consider a better model for the internal radiation, but it requires more computational effort, which is not the major interest of this study. Nevertheless, based on the same computer code, we can add a more sophisticated model for radiation if necessary.

The no-slip condition is used for the velocity at solid boundaries. At the free surface, the shear stress balance is imposed:

$$\vec{\tau} : \vec{n}\vec{s} = Ma(\partial / \partial T) \tag{5}$$

where $\vec{\tau} : \vec{n}\vec{s}$ is the shear stress at the *n*-*s* plane of the free surface; $\vec{n}$ and $\vec{s}$ are the unit normal and tangential vectors at the free surface, respectively. Also, Ma is the Marangoni number, which is defined as:

$$Ma = |\partial\gamma / \partial T| T_m D_f / \rho_m \nu_m \alpha \tag{6}$$

where $\partial\gamma/\partial T$ is the surface-tension-temperature coefficient of the melt. Two tangential directions need to be considered for the stress balance. In addition, the kinematic condition $(\vec{n} \cdot \vec{v} = 0)$ at the free surface and the normal stress balance (the Young–Laplace equation) are also satisfied, i.e.,

$$\vec{\tau} : \vec{n}\vec{n} = (2H) B_0 + \lambda_0 \tag{7}$$

where 2*H* is the mean curvature, $B_0 = \gamma / (\rho_m g D_f^2)$ is the static Bond number; g is the surface tension of the melt. The detailed way for calculating the mean curvature can be found elsewhere. Also, λ_0 is a reference head that needs to be determined to satisfy the growth angle constraint for the steady growth or the global mass conservation for stationary melting. For the steady growth, the growth angle constraint needs to be satisfied at the melt/gas/crystal tri-junction, i.e.,

$$\vec{n}_m \cdot \vec{n}_c = \cos\phi_0 \tag{8}$$

where $\vec{n}_m$ and $\vec{n}_c$ are the unit vectors at the melt and crystal surfaces, respectively, at the trijunction line ϕ_0 is the growth angle for the growing crystal having a constant local radius. However, the static head λ_0 is used to satisfy the global mass conservation,

$$A_c U_c = A_f U_f . \tag{9}$$

The thermal boundary conditions at the growth and feeding fronts are set by the heat flux balances:

$$Q|_m - Q|_i + \gamma_c (v_i \vec{e}_x) St \cdot \vec{n} = 0, \; i = (c, f) \tag{10}$$

where $\vec{n}$ is the unit normal vector at the feeding or growth interface pointing to the melt. $Q|_m$, $Q|_c$, and $Q|_f$ are the dimensionless total heat fluxes at the melt, the crystal, and the feeding sides, respectively. Also, γ_c is the density ratio of the crystal to the melt. The Stefan number $St = \Delta H / Cp_m T_m$ scales the heat of fusion ΔH released during solidification to the sensible heat in the melt; Cp_m is the specific heat of the melt. The heat transfer between the sample surface and the surrounding is similar to that in the 2D case described before.

The above governing equations and their associated boundary conditions can only be solved numerically. We have developed an efficient finite volume method (FVM) scheme using the primitive variable formulation and multigrid acceleration for the free and moving boundary problems. In the present study, YAG, steady-state results are always obtained. Two levels of grids are used. The overall iteration scheme for getting a steady-state solution is straightforward. Temperature and velocity calculations are placed in

the inner iterations. After having a number of inner iterations, we find the interface shape by locating the melting point isotherm, which also provides the position for the upper and lower tri-junction rims. Then, the meniscus is calculated based on the normal stress balance, in which there is an outer iteration loop for moving the local radii and getting the reference pressure to satisfy the growth angle or constant mass constraint and the overall mass conservation. The iterations continue until all variables converge. Detailed description of the numerical method can be found elsewhere.

3. Results and Discussion

The main mechanism of heat transfer for the micro-floating zone is thermal conduction. Therefore, the distribution of temperature field in the molten zone is basically subject to the heat input position. The temperature distribution is transfer from high-temperature isotherm to low-temperature isotherm of both solid crystal ends [3,4]. Laser heating ring deviation will cause the destruction of symmetry of temperature field, resulting in solid-liquid interface position is not symmetrical in the central axis [2]. The gravity field of the symmetry of the deviation will result in the destruction of symmetry of vapor-liquid interface. Both will affect the shape of the molten zone interface, but the mechanism and impact scale were significantly different, and the influence for the flow field within the molten zone will be also different. This experimental observation is difficult. We select YAG as a simulation material to set laser heating and gravity field deviation 3 degree from symmetry of growth axis. In 0.5 diameter reduction ratio with 500-μm-diameter source rod as the base we compare flow field influence in the molten zone caused by the two parameters perturbations to same diameter reduction ratio with 300-μm-diameter source rod and 0.25 diameter reduction ratio with same diameter source rod. The flow field distribution in x-y plane at z=0 was shown in Fig. 2, where vector is flow field velocity vector. The color bar is divided into 25 equal parts to show the highest and lowest values of axial and horizontal velocity component in the plane. When the greater the symmetry, the central axis of the pattern on both sides showed more similarity. In comparison Fig.2 (a) with (b), and (c) we can obtain that asymmetry of (a) is mainly from the effects of (b) with asymmetric laser heating ring, and slight asymmetry of gravity field has little effect to (c) at different input power level. The vector distribution in the insets showed that high laser power will lead to increase the length of the molten zone, and double vorticity has a larger deviation at the same time. Therefore it will accelerate the double vorticity tilt to increase unstable molten zone. Fig. 3 shows the simulation results with two different diameter reduction ratio and source rod diameter when the laser heating ring deviation 3 degree, where Fig. 3 (a) is captured Fig. 2 (b). It shows the influence of flow field will decrease with the source rod scale and diameter reduction ratio reducing. From the Eqs. (5) and (7), the molten zone of vapor-liquid interface shape can be formed by the normal stress of internal flow field, surface tension, and gravity field under equilibrium conditions.The main mechanisms of internal flow field stress for the micro-floating zone are mass-transfer convection, natural convection and thermocapillary convection on vapor-liquid interface, but the latter is the largest scale and the most significant impact [3,4]. It shows that the molten zone shape and flow field are not affected obviously by gravity. In order to reduce internal flow field stress the simulation parameter of thermalcapillary coefficient was reduced one order (-0.0035 $dyn.cm^{-1}.{}^{O}C^{-1}$) as shown in Fig. 4 (b). It shows that the flow field and the shape of molten zone remain symmetry. When the surface tension down to 100 $dyn.cm^{-1}$, the vapor-liquid interface has been presented convex asymmetric (the vapor-liquid interface more protruding in the gravity field direction), and indirectly affected the symmetry of the solid-liquid interface. But the double vorticity of the internal flow field is still showing nearly symmetrical situation.significant difference with double vorticity tilt caused by the slight asymmetry of laser heating ring. In other words, under suitable source rod scale and to meet tolerance of the surface tension, LHPG horizontal growth will be compensated asymmetry of the solid-liquid interface caused by larger deviation of gravity field when we slightly adjust the deviation of laser heating ring.

4. Conclusions

The main mechanism of heat transfer for the system is thermal conduction. Heat is transfer from the heating spot to the both ends.

Thermal convection of the molten zone controlled mainly by the thermocapillary convection to form double eddy flow field. The shape of molten zone can be affected by laser heating and gravity field with space asymmetrical perturbation according to the size of source rod, followed by the laser power level, and then followed by the reduction ratio. Symmetrical flow field of molten zone is symmetrical double eddy flow field. When space perturbation takes place, it will induce flow field tilt, leading to the field instability. When the size of source rod and the reduction ratio increase, the gravity field and effect of flow field stress will increase and perturbation of molten zone also increase. We know from the above analysis, the influence of flow field in the molten zone by asymmetry of the laser heating ring is much larger than the gravity field deviation. The simulation results will help us to develop the technology of LHPG with horizontal growth.

Acknowledgment

This work was supported in part by National Science Council, Taiwan, ROC, under contracts NSC-96-2221-E-019-021.

References

[1] R. S. Feigelson, Journal of Crystal Growth 79 (1986) 669.

[2] C. Y. Lo, P. Y. Chen, International Conference on Materials for Advanced Technologies, paper DD3-6, Suntec, Singapore (2011).

[3] P. Y. Chen, C. L. Chang, K. Y. Huang, C. W. Lan, W. H. Cheng, S. L. Huang, Japanese Journal of Applied Physics 48 (2009) 115504

[4] P. Y. Chen, C. L. Chang, K. Y. Huang, C. W. Lan, W. H. Cheng, S. L. Huang, Journal of Applied Crystallography 42 (2009) 553.

[5] C. L. Chang, S. L. Huang, C. Y. Lo, K. Y. Huang, C. W. Lan, W. H. Cheng, P. Y. Chen, Journal of Crystal Growth 318 (2011) 674.

[6] C. W. Lan, B. C. Yeh, Journal of Crystal Growth 262 (2004) 59.

[7] C. W. Lan, J. H. Chian, Journal of Crystal Growth 230 (2001) 172.

[8] C. W. Lan, Journal of Crystal Growth 247 (2003) 597.

[9] C. W. Lan, C. Y. Tu, Journal of Crystal Growth 223 (2001) 523.

Figure Captions:

Fig. 1. Three-dimensional view of LHPG method, where D_f and D_c are the source rod diameter and seed diameter, respectively.

Fig. 2. The influence of flow field distribution in the molten zone caused by (a) laser heating and gravity field deviation 3^0, (b) laser heating deviation 3^0, (c) gravity field deviation 3^0 to the growth axis. The diameter of source rod and reduction ratio are 500 μm and 0.5, respectively.

Fig. 3. The influence of flow field distribution in the molten zone caused by laser heating deviation 3^0 to the growth axis under different simulation conditions of (a) D_f =500 μm, r = 0.5, (b) D_f =500 μm, r = 0.25, (c) D_f =300 μm, r = 0.5, where r is the diameter reduction ratio.

Fig. 4. The influence of flow field distribution in the molten zone caused by gravity field deviation 90^0 to the growth axis under different simulation conditions of (a) γ= 780,t_c= - 0.035 , (b) γ= 780,t_c= - 0.0035 (c) γ= 100, t_c= - 0.035, where γ and t_c are surface tension and thermalcapillary coefficient, respectively. The diameter of source rod is 1000 μm.

Table(s)

Table 1. Physical properties of YAG and related input parameters

Symbols	Values	Units	Descriptions
	Yttrium aluminum garnet; YAG		
ρ_s	3.685	$g \cdot cm^{-3}$	Density of solid
ρ_m	4.3	$g \cdot cm^{-3}$	Density of melt
T_m	1970.0	°C	Melting point
ΔH	455.5	$J \cdot g^{-1}$	Melt/solid latent heat
k_s	0.1	$W \cdot cm^{-1} \cdot °C^{-1}$	Thermal conductivity of solid*
k_m	0.1	$W \cdot cm^{-1} \cdot °C^{-1}$	Thermal conductivity of melt*
C_{ps}	1.0	$J \cdot g^{-1} \cdot °C^{-1}$	Specific heat of solid*
C_{pm}	0.39	$J \cdot g^{-1} \cdot °C^{-1}$	Specific heat of melt*
$\partial\gamma/\partial T$	-0.035	$dyn \cdot cm^{-1} \cdot °C^{-1}$	Surface-tension-temperature coefficient*
γ	780	$dyn \cdot cm^{-1}$	Surface tension*
μ_m	0.4	$g \cdot cm^{-1}s^{-1}$	Viscosity of melt
β_m	6.5×10^{-5}	K^{-1}	Thermal expansion coefficient of melt
ε_s	0.7	—	Radiation emissivity of solid
ε_m	0.5	—	Radiation emissivity of melt
	Other input parameters		
$D_{s,c}$	See Table IV	μm	Diameters of rod and fiber
$U_{s,c}$	See Table IV	μm/s	Speeds of feed and growth
L	5	cm	Rod length
h	1.1×10^{-3}	$W \cdot cm^{-2} \cdot K^{-1}$	Heat transfer coefficient
f_m	1.00~1.88	—	Factor of equivalent melt absorption
a_m	0.5	—	Gray body factor

*at melting point

Figure(s)

Fig. 1

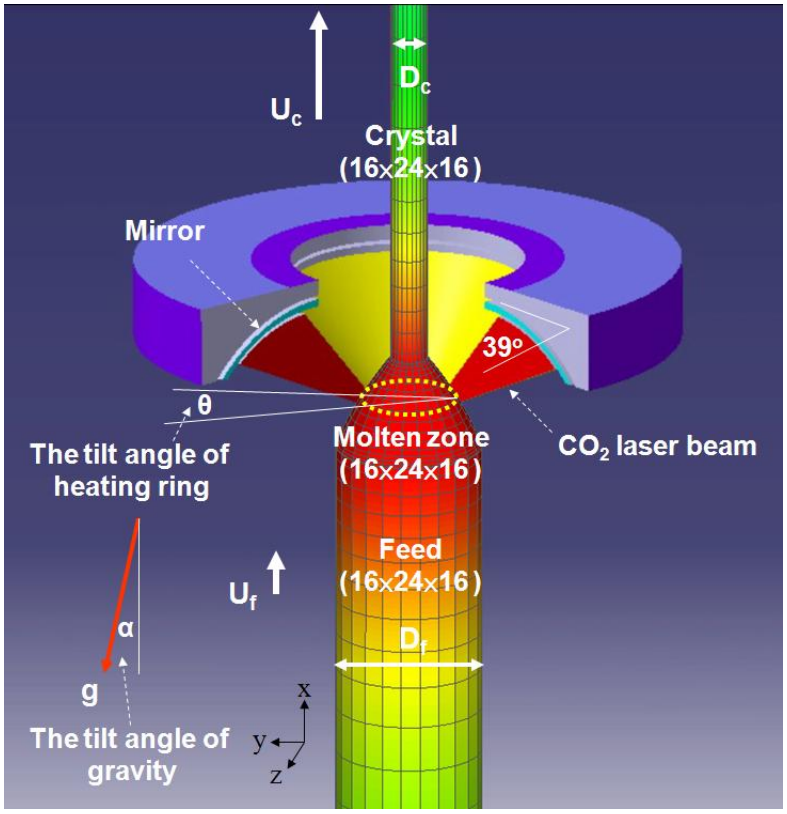

Fig. 2

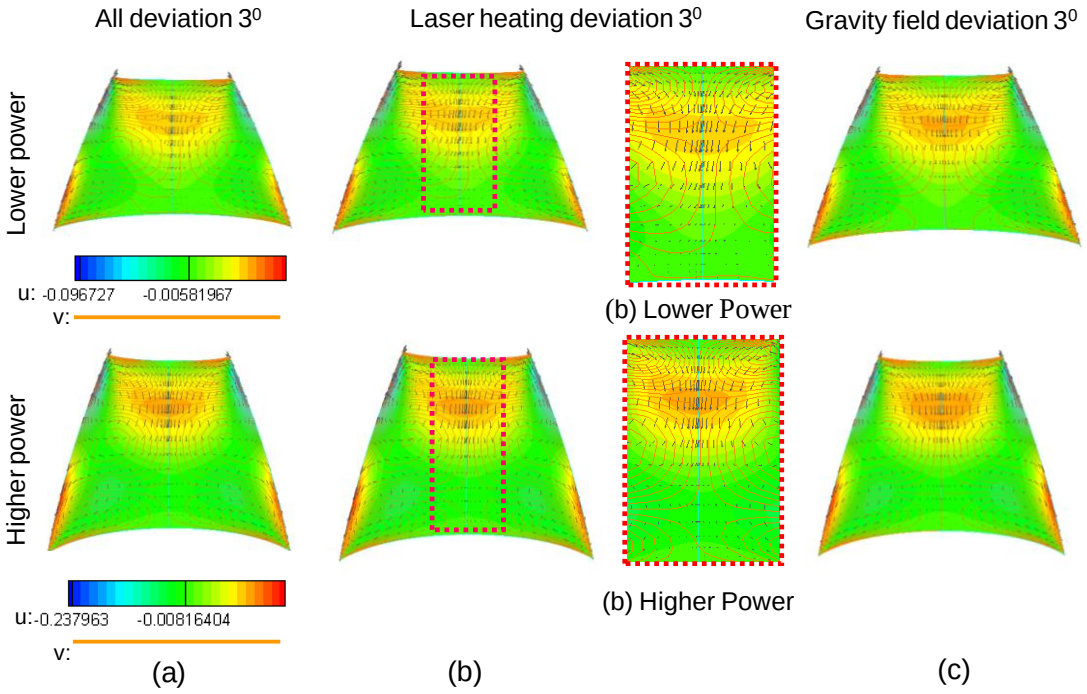
All deviation 3⁰
Laser heating deviation 3⁰
Gravity field deviation 3⁰
Lower power
u: -0.096727 -0.00581967
v:
(b) Lower Power
Higher power
u: -0.237963 -0.00816404
v:
(b) Higher Power
(a)
(b)
(c)

Fig. 3

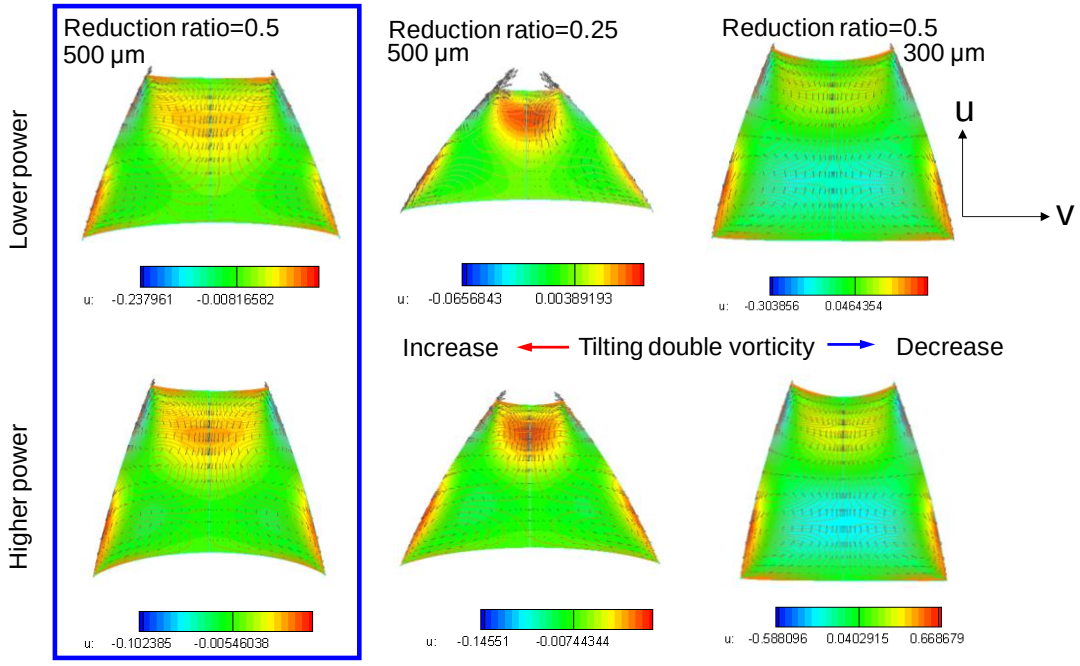
Reduction ratio=0.5
500 μm
Reduction ratio=0.25
500 μm
Reduction ratio=0.5
300 μm
Lower power
Higher power
u
v
u: -0.237961 -0.00816582
u: -0.0656843 0.00389193
u: -0.303856 0.0464354
Increase
Tilting double vorticity
Decrease
u: -0.102385 -0.00546038
u: -0.14551 -0.00744344
u: -0.588096 0.0402915 0.668679
(a)
(b)
(c)

Fig. 4

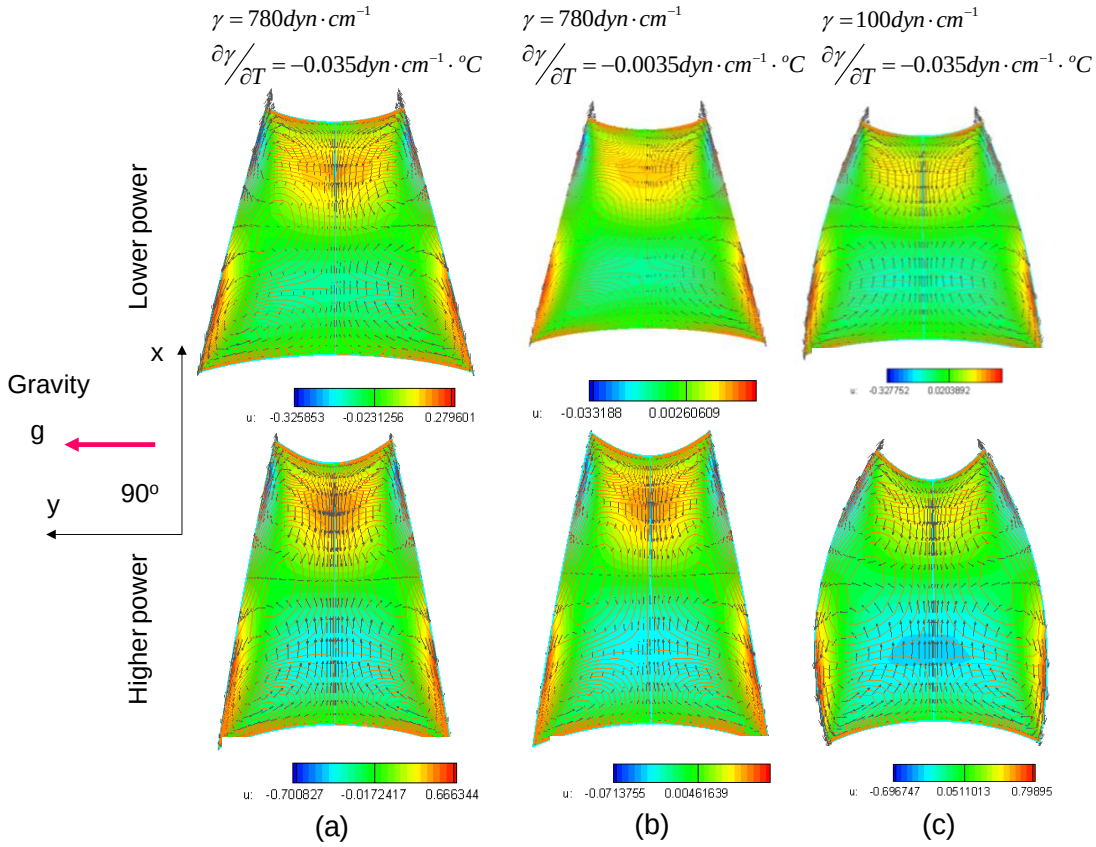
$\gamma = 780 dyn \cdot cm^{-1}$
$\partial\gamma/\partial T = -0.035 dyn \cdot cm^{-1} \cdot {}^{o}C$
$\gamma = 780 dyn \cdot cm^{-1}$
$\partial\gamma/\partial T = -0.0035 dyn \cdot cm^{-1} \cdot {}^{o}C$
$\gamma = 100 dyn \cdot cm^{-1}$
$\partial\gamma/\partial T = -0.035 dyn \cdot cm^{-1} \cdot {}^{o}C$
Lower power
x
Gravity
g
90°
y
Higher power
u: -0.325853 -0.0231256 0.279601
u: -0.033188 0.00260609
u: -0.700827 -0.0172417 0.666344
u: -0.0713755 0.00461639
u: -0.696747 0.0511013 0.79895
(a)
(b)
(c)